November 1994 Chem. Pharm. Bull. 42(11) 2269—2275 (1994)

Studies on Chemical Modification of Monensin. V. Synthesis, Sodium Ion Permeability, Antibacterial Activity, and Crystal Structure of 7-*O*-(4-Substituted benzyl)monensins

Akito NAGATSU (née NAKAMURA), Tadashi TAKAHASHI, Miki ISOMURA, Shin-ichi NAGAI, Taisei UEDA, Nobutoshi MURAKAMI, Jinsaku SAKAKIBARA,* and Keiichiro HATANO

Faculty of Pharmaceutical Sciences, Nagoya City University, Mizuho-ku, Nagoya 467, Japan.

Received June 30, 1994; accepted July 21, 1994

7-*O*-(4-Substituted benzyl)monensins (3a—g) were synthesized from monensin (1), and their lipophilicity, antibacterial activity, and Na^+ ion permeability were examined. 7-*O*-(4-Ethylbenzyl)monensin (3e) showed the largest Na^+ ion permeability, but 3c,f,g showed smaller Na^+ ion permeability than 7-*O*-benzylmonensin (2) in spite of higher lipophilicity. An X-ray study of the sodium salt of 3e revealed that the benzyl group was located over the position between the D and E rings, and that the ethyl substituent on the benzyl group was close to the C(28) methyl group on the E ring.

Keywords monensin; 7-*O*-(4-substituted benzyl)monensin; lipophilicity; sodium ion permeability; antibacterial activity; crystal structure

Monensin (**1**, Chart 1), a polyether isolated from *Streptomyses cinnamonensis*, is a very potent antibiotic and anticoccidial agent.[1] The Na^+ salt of monensin (**1**) has a cyclic conformation[2] with the carboxylic oxygens at one end hydrogen-bonded to the hydroxyls at the other end. The molecule as a whole is therefore lipophilic enough to transport Na^+ ion across the lipophilic biological membrane. In a previous study,[3] we modified the C-7 hydroxyl group, which is appended to the periphery of the microcyclic structure, in order to obtain more lipophilic compounds than monensin (**1**). We found that 7-*O*-benzylmonensin (**2**) has higher lipophilicity and larger Na^+ ion permeability than those of **1**. We then became interested in introducing substituents onto the benzyl group, which would affect the lipophilicity and Na^+ ion permeability. In this paper, we report the synthesis of 7-*O*-(4-substituted benzyl)monensins (**3**), and measurement of their lipophilicity and Na^+ ion permeability as well as antibacterial activity. We also carried out an X-ray crystal structure analysis of **3e** in order to clarify the effects of the 4-substituted benzyl groups.

Results

Chemistry The synthesis of compounds (**3**) was carried out by essentially the same method as described before[3] (Chart 2). The diol group at the 25 and 26 positions and the carboxyl group of **1** were protected with a 4-methoxybenzylidene acetal group and a methyl ester, respectively, to give **4**. This compound (**4**) was warmed with NaH at 50 °C for 30 min in tetrahydrofuran (THF) followed by treatment with appropriate 4-substituted benzyl iodides[4] to yield a mixture of the corresponding **5a**—**g** and olefinic by-products (**6a**—**g**) in the ratio indicated in Table I. The separation of **5a**—**g** and **6a**—**g** was not carried out at this step. Hydrolysis of methyl esters of the mixtures followed by cleavage of 4-methoxybenzylidene acetals gave the desired monensin derivatives (**3a**—**g**) after separation of the reaction mixture by preparative TLC and medium-pressure liquid chromatography.

The lipophilicity of the compounds (**3a**—**g**) was determined by measuring *Rm* values.[5] Benzyl derivatives (**3b**—**g**) showed higher lipophilicity than **2** (Table II). The compounds (**3a**—**g**) having a larger substituent at the 4 position of the benzyl group exhibited higher lipophilicity.

Na^+ Ion Permeability The Na^+ ion permeability of the compounds in a biological membrane was determined by measuring intracellular Na^+ ion concentration ($[Na_{in}]$), using a ^{23}Na-NMR method as described before.[3,6] We used erythrocyte suspension in medium containing 140 mM Na^+, 5 mM K^+ and a test compound (10^{-6} M). Compounds **3a**—**g** as well as **1** and **2** initially caused a rapid increase of $[Na_{in}]$ and then the rate gradually slowed down to reach a plateau (Fig. 1). Figure 2 shows the increase of $[Na_{in}]$ within the first 5 min ($\Delta[Na_{in}]^5$), which is considered to be represent the initial rate of increase of $[Na_{in}]$; this is an important indicator of the Na^+ ion permeability of the compounds. All of **3** showed larger $\Delta[Na_{in}]^5$ than **1**, and the $\Delta[Na_{in}]^5$ values of **3b** and **3d**—**f** are larger than that of **2**. Compound **3e** showed the largest $\Delta[Na_{in}]^5$, which is twice the value of

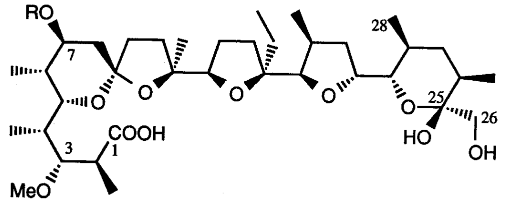

monensin (**1**) R=H
7-*O*-benzylmonensin (**2**) R=$CH_2C_6H_5$
7-*O*-(4-substituted benzyl)monensins (**3**) R=CH_2-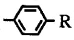-R^1

a: R^1=F **d**: R^1=Me
b: R^1=Cl **e**: R^1=Et
c: R^1=Br **f**: R^1=iso-Pr
g: R^1=*tert*-Bu

Chart 1

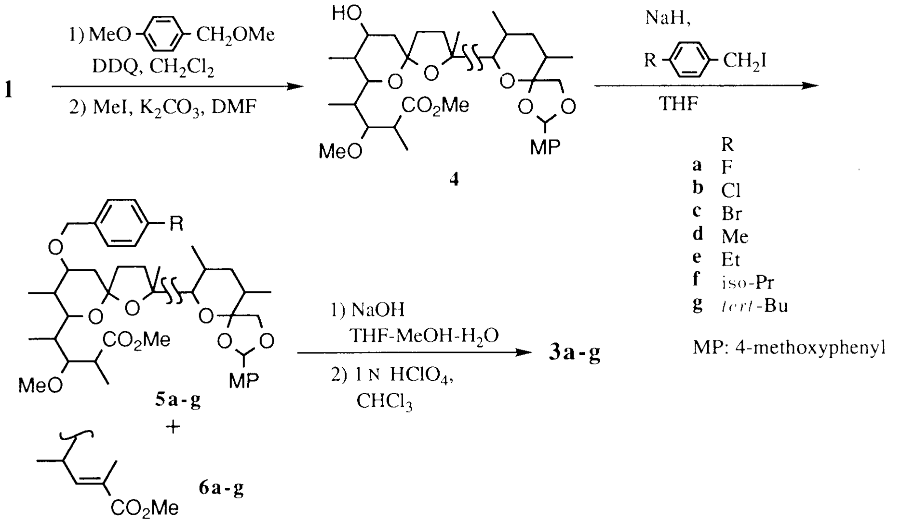

Chart 2

Table I. Reaction Times and Yields of 7-*O*-Benzylation

5+**6**	R	Reaction time (h)	Yield of **5**+**6** (%)	Ratio of **5**:**6**[a]
a	F	10	82	3:1
b	Cl	9	91	10:1
c	Br	9	85	3:1
d	Me	11	81	5:1
e	Et	8	77	3:1
f	iso-Pr	7	73	3:1
g	*tert*-Bu	7	69	2:1

[a] The ratio was determined by ^{1}H-NMR.

Table II. Rm_{50} Values of 7-*O*-(4-Substituted benzyl)monensins (**3a**—**g**), Monensin (**1**) and **2**

Compound	Rm_{50}	Compound	Rm_{50}
1	1.81	**3d**	2.26
2	2.04	**3e**	2.41
3a	2.00	**3f**	2.55
3b	2.17	**3g**	2.67
3c	2.21		

1 and about 1.4 times the value of **2**.

Antibacterial Activity The values of minimum inhibitory concentration (MIC) against various bacteria were measured by the agar dilution method. All 7-*O*-(4-substituted benzyl)monensins (**3a**—**g**) had stronger antibacterial activity than monensin (**1**) (Table III). All the compounds (**3a**—**g**) gave almost the same MIC values.

X-Ray Crystal Structure Analysis We attempted an X-ray crystal structure analysis of the sodium salt of **3e** (Na-**3e**), which showed the largest Na^+ ion permeability. Since it was difficult to obtain directly the structural solution of Na-**3e**, we made use of the K^+ salt of **3e** (K-**3e**), which crystallized isomorphously with Na-**3e**. The structure of K-**3e** was solved first, then the structure of Na-**3e** was solved successfully by use of the atomic positions of K-**3e**, as described in the experimental section. The molecular diagram and numbering of the atoms of **3e** are shown in Fig. 3. The structures of Na-**3e** and K-**3e** were essentially the same, as expected, and stereoviews are shown in Fig. 4. The pseudocyclic structures of these salts were very similar to those of the corresponding salts of monensin (**1**) with respect to the atomic geometry, including head-to-tail hydrogen bonds and ion coodinations (Table IV). A notable exception is that the atomic

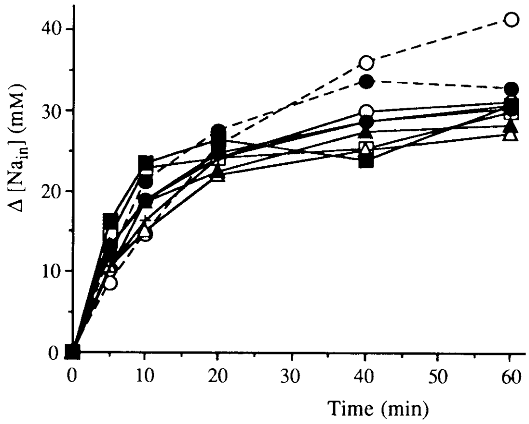

Fig. 1. Time Course of Δ [Na$_{in}$] of 7-*O*-(4-Substituted benzyl)monensins (**3a**—**g**), Monensin (**1**), and **2**

---○---, **1**; ---●---, **2**; ○, **3a**; □, **3b**; △, **3c**; ●, **3d**; ■, **3e**; ▲, **3f**; —+—, **3g**.

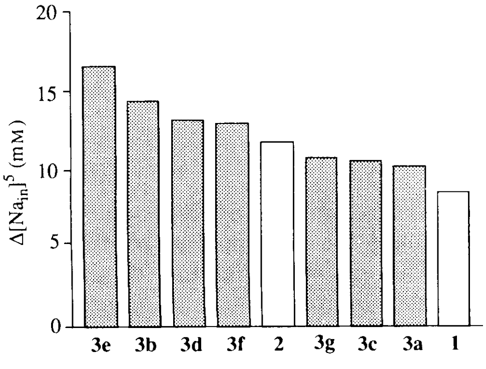

Fig. 2. $\Delta[Na_{in}]^5$ of 7-*O*-(4-Substituted benzyl)monensins (**3a**—**g**), Monensin (**1**), and **2**

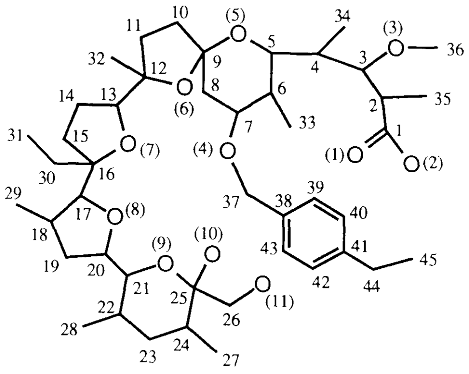

Fig. 3. Atomic Numbering of **3e**

distance of Na–O(4) of Na-**3e** is about 10% longer than that of monensin sodium. The benzyl group of **3e** covers the hydrophilic central cavity and extends over the position between the D and E rings. The ethyl group at the 4 position of the benzyl group is located outside of the pseudocyclic ring of the molecule. These structural features will be discussed below.

Discussion

The ^{1}H-NMR spectra of **3a**—**g** as well as **2** showed doublet methyl signals of 28-H_3 at δ 0.11—0.21 ppm. The signals of 20-H and 21-H of **2** and **3a**—**g** also appeared at significantly higher field than those of monensin (**1**) (Table

Table III. Antibacterial Activity of 7-*O*-(4-Substituted benzyl)monensin (**3a**—**g**), Monensin (**1**), and **2**

Bacterias	MIC (μg/ml)								
	1	**2**	**3a**	**3b**	**3c**	**3d**	**3e**	**3f**	**3g**
Peptostreptococcus anaerobius ATCC 27337	0.78	0.20	0.05	0.10	0.10	0.10	0.20	0.20	0.10
Propionibacterium acnes ATCC 6919	0.78	0.39	0.39	0.20	0.39	0.20	0.39	0.39	0.10
Lactobacillus acidophilus ATCC 4356	6.25	0.39	0.78	0.20	0.78	0.78	0.39	0.78	1.56
Lactobacillus salivarius ATCC 11741	6.25	0.39	0.78	0.39	0.78	0.78	0.78	0.78	1.56
Clostridium perfringens NCTC 4969	6.25	0.39	0.78	0.78	0.78	0.78	0.39	0.39	0.78
Eubacterium lentum GAI 7506	0.20	0.10	0.10	0.05	0.10	0.10	0.05	0.10	0.05
Staphylococcus aureus 209P-JC	0.78	0.20	0.05	0.20	0.10	0.20	0.10	0.39	0.39
Staphylococcus epidermidis IID 866	0.78	0.20	0.20	0.20	0.10	0.20	0.20	0.10	0.39
Bacillus subtilis ATCC 6633	0.39	0.20	0.10	0.20	0.10	0.20	0.10	0.10	0.20

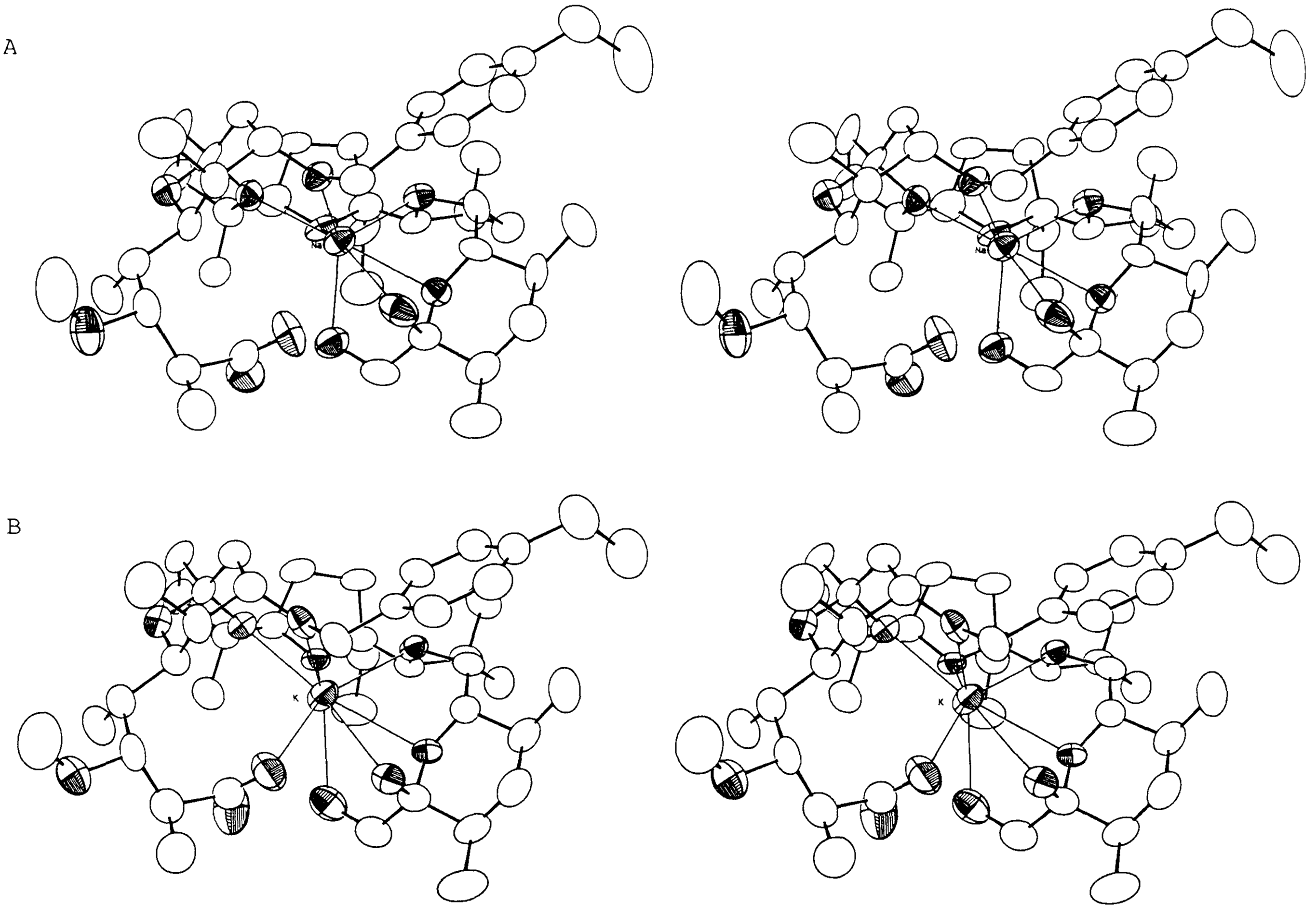

Fig. 4. Stereoviews of Na-**3e** (A) and K-**3e** (B) with Thermal Ellipsoids at 50% Probability for Non-hydrogen Atoms

Octant-shaded ellipsoids are oxygens. Atoms of the solvent molecule and the disordered part, and all hydrogens are omitted for clarity.

Table IV. Atomic Distances

Atoms	Distance (Å)			
	Na$^+$ salt		K$^+$ salt	
	3e	**1**[7]	**3e**	**1**[8]
Hydrogen bonds				
O(1)–O(10)	2.62	2.64	2.72	2.62
O(2)–O(11)	2.54	2.51	2.59	2.51
Ion coordination				
M–O(4)	2.585 (9)	2.346 (2)	2.695 (6)	2.650
M–O(6)	2.394 (9)	2.411 (2)	2.627 (5)	2.660
M–O(7)	2.490 (9)	2.529 (2)	2.764 (6)	2.785
M–O(8)	2.477 (9)	2.408 (2)	2.717 (7)	2.717
M–O(9)	2.543 (9)	2.513 (2)	2.798 (6)	2.796
M–O(11)	2.40 (1)	2.381 (2)	2.712 (7)	2.786
Nonbonding carbon–carbon distances (<4 Å)				
C(20)–C(39)	3.770	—	—	—
C(21)–C(38)	3.950	—	—	—
C(21)–C(39)	3.786	—	3.799	—
C(28)–C(45)	3.933	—	3.402	—

Table V. ^{1}H-NMR Chemical Shifts of 20-H, 21-H, and 28-H_3 of Na$^+$ Salts of **1**, **2**, and **3a**—**g**

Compound	R	δ (ppm)		
		20-H	21-H	28-H_3
1	—	4.38	3.82	0.80
2	H	3.89	3.40	0.13
3a	F	3.94	3.41	0.21
3b	Cl	3.94	3.40	0.21
3c	Br	3.95	3.40	0.21
3d	Me	3.98	3.47	0.20
3e	Et	3.91	3.46	0.16
3f	iso-Pr	3.84	3.37	0.13
3g	*tert*-Bu	3.79	3.40	0.11

V). These phenomena were probably due to the anisotropic effect of the benzene ring, and indicated that benzyl groups were close to the C(20), C(21), and C(28) positions. Although no nuclear Overhauser effect (NOE) was observed between protons at these carbons and at the benzyl group of the Na$^+$ and K$^+$ salts of **3**, the crystal structure of Na-**3e** revealed that the benzyl group was actually in the vicinity of C(20), C(21), and C(28) (Table IV), and that 20-H, 21-H and 28-H_3 were located above the benzene ring and were magnetically shielded.

Although the substitution of the 7-*O* position with various benzyl groups led to higher lipophilicity of the molecules, the more lipophilic compounds such as **3c**, **f**, **g** showed smaller Na$^+$ ion permeability than **3e**. In comparison with the conformations of Na-**3e** and the sodium salt of monensin (**1**)[7] (Fig. 5), the E ring of **3e** is shifted in the opposite direction to the benzyl group. This fact and the longer Na–O(4) distance of Na-**3e** implies steric repulsion between the E ring and the benzyl group. Considering the spatial volumes occupied by the protons at C(28) and C(45), the ethyl substituent on the benzyl group was the nearest to the E ring. Bulkier substituents than the ethyl group should cause larger steric repulsion which would induce slower Na$^+$ ion complexation and release and/or reduced stability of the sodium complex. Compounds **3a**—**d**, **f**, **g** should have similar conformations to Na-**3e** in a lipophilic environment, because ^{1}H-NMR of **3a**—**g** exhibited high field shifts of the signals due to 20-H, 21-H and 28-H_3 in lipophilic $CDCl_3$. Thus, **3c**, **f**, **g**, the compounds with larger substituents on the benzyl groups, have smaller Na$^+$ ion permeability than **3e** in spite of larger lipophilicity.

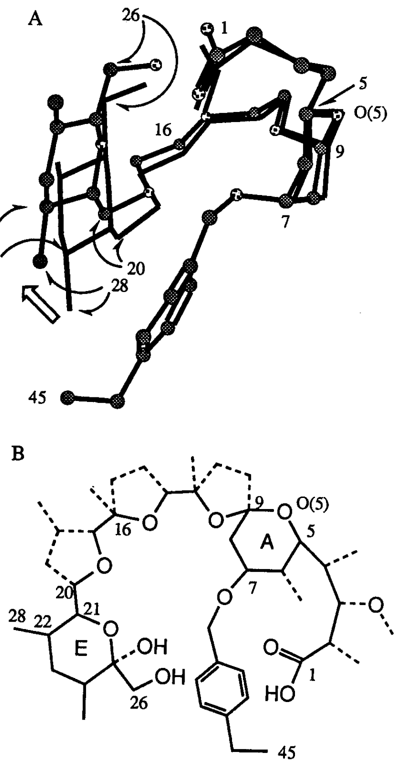

Fig. 5. Comparison of the Structures of Na-**3e** and Monensin Sodium

The structure of Na-**3e** (ball and stick model) was superimposed on that of monensin sodium[7] (wire model), then the C(5)–O(5) bond was subjected to fitting. (A) The structures are illustrated by the bonds indicated by solid lines in structure B.

In summary, we synthesized 7-*O*-(4-substituted benzyl) monensins (**3a**—**g**), and found that the substitution induced higher lipophilicity of the molecules. Compound **3e** showed the largest Na$^+$ ion permeability. From the result of X-ray crystal structure analysis of **3e**, the ethyl group on the benzene ring was placed very close to C(28) on the E ring. This fact suggested that larger substituents at the *para* position of the benzyl group would cause steric repulsion. This information will be of benefit in design of more useful ionophores based on monensin.

Experimental

All melting points were determined on a Yanagimoto micro melting point apparatus and are uncorrected. The FAB-MS were measured with a JEOL JMS DX-300 mass spectrometer, and the IR spectra with a JASCO IRA-2 spectrometer. The ^{1}H-NMR spectra were measured with a JEOL GSX-400 spectrometer using tetramethylsilane as an internal standard. The following abbreviations are used; s, singlet; d, doublet; dd, doublet-of-doublets; m, multiplet. Optical rotations were measured on a JASCO DIP-140 digital polarimeter. Medium-pressure liquid chromatography was carried out on C.I.G. ODS-C_{18}-10/20 (22 mm i.d. × 100 mm, Kusano Kagakukikai Co.) using a Kusano KPW-20 pump and KU-331 UV detector. TLC was carried out on precoated plates (Kieselgel 60F_{254}, 0.25 mm thick, Merck no. 5715), and spots were detected by illumination with an ultraviolet lamp or 1% $Ce(SO_4)_2$–10%

H_2SO_4, followed by heating. Column chromatography was performed on Silica gel BW-200 (Fuji Davison Chemicals Co., Ltd.).

General Procedure for Preparation of 7-*O*-(4-Substituted benzyl)monensins (3a—g) A solution of **4** (200 mg) in THF (6 ml) was stirred in the presence of NaH (5 eq) at 50 °C for 30 min. The mixture was cooled to room temperature, and 4-fluorobenzyl iodide (5 eq) in THF was added. The mixture was stirred in the dark at room temperature for 3 h. The reaction was quenched by the addition of NH_4Cl solution and the mixture was diluted with AcOEt. The organic layer was washed with brine, dried over $MgSO_4$, filtered, and evaporated to dryness. The residue was chromatographed on silica gel (hexane–ether) to give a mixture of **5a** and **6a** (185 mg) as a syrup in the ratio of 3 : 1.

Table VI. Spectral Data for **5**+**6**

5+6	IR (KBr) of C=O, cm^{-1}	^1H-NMR ($CDCl_3$) δ (ppm)
a	1735	3.33 (s, 3-OCH_3), 3.46 (1H, m, 7-H), 3.51 (3H, s, CO–OCH_3), 3.81 (3H, s, Ar-OCH_3), 4.40 4.61 (each 1H, both d, J=11.9 Hz, 7-OCH_2–), 6.57 (d, 3-H of **6a**)
b	1735	3.33 (s, 3-OCH_3), 3.46 (1H, m, 7-H), 3.52 (3H, s, CO–OCH_3), 3.83 (3H, s, Ar-OCH_3), 4.42, 4.61 (each 1H, both d, J=12.1 Hz, 7-OCH_2–), 6.57 (d, 3-H of **6b**)
c	1735	3.33 (s, 3-OCH_3), 3.46 (1H, m, 7-H), 3.52 (3H, s, CO–OCH_3), 3.81 (3H, s, Ar-OCH_3), 4.40, 4.59 (each 1H, both d, J=12.3 Hz, 7-OCH_2–), 6.57 (d, 3-H of **6c**)
d	1735	3.33 (s, 3-OCH_3), 3.47 (1H, m, 7-H), 3.55 (3H, s, CO–OCH_3), 3.81 (3H, s, Ar-OCH_3), 4.41, 4.61 (each 1H, both d, J=11.9 Hz, 7-OCH_2–), 6.58 (d, 3-H of **6d**)
e	1735	3.33 (s, 3-OCH_3), 3.45 (1H, m, 7-H), 3.54 (3H, s, CO–OCH_3), 3.81 (3H, s, Ar-OCH_3), 4.42, 4.62 (each 1H, both d, J=12.2 Hz, 7-OCH_2–), 6.59 (d, 3-H of **6e**)
f	1735	3.33 (s, 3-OCH_3), 3.45 (1H, m, 7-H), 3.53 (3H, s, CO–OCH_3), 3.81 (3H, s, Ar-OCH_3), 4.42, 4.62 (each 1H, both d, J=11.9 Hz, 7-OCH_2–), 6.59 (d, 3-H of **6f**)
g	1735	3.33 (s, 3-OCH_3), 3.45 (1H, m, 7-H), 3.54 (3H, s, CO–OCH_3), 3.81 (3H, s, Ar-OCH_3), 4.42, 4.62 (each 1H, both d, J=12.0 Hz, 7-OCH_2–), 6.59 (d, 3-H of **6g**)

A solution of a mixture of **5a** and **6a** (170 mg) in THF–MeOH–H_2O (2 : 2 : 1, 3 ml) containing 1 N NaOH was stirred at room temperature for 6 h and extracted with AcOEt. The extract was washed with brine, dried over $MgSO_4$, and evaporated to dryness to give the residue (164 mg). The residue (150 mg) was taken up in $CHCl_3$ (3 ml), then 1 N $HClO_4$ aqueous solution was added and the whole was stirred vigorously at room temperature for 3 h. The $CHCl_3$ layer was shaken with 4% $NaHCO_3$, dried over Na_2SO_4, and evaporated to dryness. The residue was purified by preparative TLC on silica gel ($CHCl_3$–MeOH) followed by reversed-phase medium-pressure liquid chromatography (MeOH–H_2O) to give the sodium salt of **3a** (71 mg, 42 % from **4**) as a syrup. The other 7-*O*-(4-substituted benzyl)monensins (**3b**—**g**) were similarly obtained from **4**. The reaction times and yields of **5b**—**g** and **6b**—**g** are indicated in Table I. The spectral data of **5** and **6** are summarized in Table VI. The spectral and physicochemical data of the sodium salt of **3a**—**g** are summarized in Table VII and Table VIII. **3a**: 7-*O*-(4-fluorobenzyl)monensin; **3b**: 64% (from **4**), 7-*O*-(4-chlorobenzyl)monensin; **3c**: 44% (from **4**), 7-*O*-(4-bromobenzyl)monensin, **3d**: 49% (from **4**), 7-*O*-(4-methylbenzyl)monensin; **3e**: 43% (from **4**), 7-*O*-(4-ethylbenzyl)monensin; **3f**: 39% (from **4**), 7-*O*-(4-iso-propylbenzyl)monensin, **3g**: 34% (from **4**), 7-*O*-(4-*tert*-butylbenzyl)monensin.

***Rm* Values** The *Rm* values were measured by the method described in our previous paper[3)] using precoated TLC plates (Kieselgel $60F_{254}$ silanized, 0.25 mm thick, Merck no. 5747).

Determination of Na^+ Ion Permeability in Erythrocyte Membrane Na^+ ion permeability in human erythrocyte membrane was measured by essentially the same method as we have reported, using ^{23}Na-NMR.[3)] ^{23}Na-NMR spectra were recorded using a JEOL EX-270 spectrometer at 71.32 MHz and 37 °C. The tube combination (1 mm o.d. tube inside a 5 mm o.d. NMR tube) contained 0.45 ml of human erythrocyte suspension, 0.05 ml of 100 mM dysprosium triethylenetetramine hexacetate in water, and 5 μl of monensin derivative in dimethyl sulfoxide (DMSO) in the annular space. The inner tube contained an external reference (20 mM dysprosium sodium triphosphate, $Na_7Dy(PPPi)\cdot 3NaCl$). The human erythrocyte suspension was prepared in a medium containing 140 mM NaCl and 5 mM KCl at pH 7.4, and hematocrit was set at 0.4. The intracellular Na^+ ion concentrations were calculated by using the reported equation.[3)]

Crystal Structure Determination and Refinement X-Ray quality single crystals of K-**3e** and Na-**3e** were obtained by slow evaporation from solutions of acetone–hexane and isopropyl ether, respectively. The crys-

Table VII. Spectral Data for Sodium Salts of 7-*O*-(4-Substituted benzyl)monensins (**3a**—**g**)

3	FAB-MS m/z	IR (KBr) of C=O, cm^{-1}	^1H-NMR ($CDCl_3$), δ (ppm)
a	801 $(M+Na)^+$, 823 $(M+2Na-H)^+$	1560	0.21 (3H, d, J=5.9 Hz, 28-H_3), 3.27, 3.92 (each 1H, both d, J=11.7 Hz, 26-H_2), 3.29 (1H, m, 7-H), 3.40 (3H, s, 3-OCH_3), 3.41 (1H, m, 21-H), 3.94 (1H, m, 20-H), 4.46, 5.96 (each 1H, both d, J=16.1 Hz, 7-OCH_2–), 7.03 (2H, dd, J=8.6, 8.6 Hz, 40-H, 42-H), 7.30 (2H, dd, J=8.6, 5.5 Hz, 39-H, 43-H)
b	817 $(M+Na)^+$, 839 $(M+2Na-H)^+$	1560	0.21 (3H, d, J=5.9 Hz, 28-H_3), 3.27, 3.92 (each 1H, both d, J=11.7 Hz, 26-H_2), 3.28 (1H, m, 7-H), 3.40 (1H, m, 21-H), 3.40 (3H, s, 3-OCH_3), 3.94 (1H, m, 20-H), 4.45, 5.98 (each 1H, both d, J=16.1 Hz, 7-OCH_2–), 7.28, 7.31 (each 2H, both d, J=8.5 Hz, Ar-H)
c	861 $(M+Na)^+$, 883 $(M+2Na-H)^+$	1560	0.21 (3H, d, J=5.9 Hz, 28-H_3), 3.27, 3.92 (each 1H, both d, J=11.8 Hz, 26-H_2), 3.28 (1H, m, 7-H), 3.38 (1H, m, 21-H), 3.40 (3H, s, 3-OCH_3), 3.95 (1H, m, 20-H), 4.43, 5.97 (each 1H, both d, J=16.1 Hz, 7-OCH_2–), 7.22, 7.46 (each 2H, both d, J=8.4 Hz, Ar-H)
d	797 $(M+Na)^+$, 819 $(M+2Na-H)^+$	1565	0.20 (3H, d, J=5.5 Hz, 28-H_3), 3.27, 3.92 (each 1H, both d, J=11.7 Hz, 26-H_2), 3.32 (1H, m, 7-H), 340 (3H, s, 3-OCH_3), 3.47 (1H, m, 21-H), 3.98 (1H, m, 20-H), 4.43, 5.94 (each 1H, both d, J=16.0 Hz, 7-OCH_2–), 7.13, 7.22 (each 2H, both d, J=7.8 Hz, Ar-H)
e	811 $(M+Na)^+$, 833 $(M+2Na-H)^+$	1560	0.16 (3H, d, J=5.5 Hz, 28-H_3), 3.27, 3.92 (each 1H, both d, J=11.7 Hz, 26-H_2), 3.34 (1H, m, 7-H), 3.40 (3H, s, 3-OCH_3), 3.46 (1H, m, 21-H), 3.91 (1H, m, 20-H), 4.46, 5.96 (each 1H, both d, J=16.1 Hz, 7-OCH_2–), 7.15, 7.22 (each 2H, both d, J=7.9 Hz, Ar-H)
f	825 $(M+Na)^+$, 847 $(M+2Na-H)^+$	1560	0.13 (3H, d, J=5.7 Hz, 28-H_3), 3.26, 3.91 (each 1H, both d, J=11.9 Hz, 26-H_2), 3.36 (1H, m, 7-H), 3.37 (1H, m, 21-H), 3.41 (3H, s, 3-OCH_3), 3.84 (1H, m, 20-H), 4.43, 5.94 (each 1H, both d, J=16.0 Hz, 7-OCH_2–), 7.18, 7.24 (each 2H, both d, J=9.2 Hz, Ar-H)
g	839 $(M+Na)^+$, 861 $(M+2Na-H)^+$	1560	0.11 (3H, d, J=5.7 Hz, 28-H_3), 3.26, 3.91 (each 1H, both d, J=11.7 Hz, 26-H_2), 3.33 (1H, m, 21-H), 3.37 (1H, m, 7-H), 3.41 (3H, s, 3-OCH_3), 3.79 (1H, m, 20-H), 4.48, 6.00 (each 1H, both d, J=16.3 Hz, 7-OCH_2–), 7.25, 7.34 (each 2H, both d, J=8.2 Hz, Ar-H)

TABLE VIII. Physicochemical Data for Sodium Salts of 7-*O*-(4-Substituted benzyl)monensins (**3a**—**g**)

3	$[\alpha]_D^{27}$ (CHCl$_3$) (*c*)	mp (°C)[a]	Formula	Calcd (Found)	
				C	H
a	+40.4 (0.37)	225—228[b]	$C_{43}H_{66}O_{11}FNa$	64.48	8.31
				(64.48	8.37)
b	+36.8 (0.59)	221—223[b]	$C_{43}H_{66}O_{11}ClNa$	63.18	8.14
				(63.25	8.23)
c	+31.6 (0.33)	210—213[b]	$C_{43}H_{66}O_{11}BrNa$	59.92	7.72
				(60.33	7.91)
d	+40.0 (0.54)	213—215[c]	$C_{44}H_{69}O_{11}Na$	66.31	8.73
				(66.61	8.82)
e	+32.3 (0.30)	213—215[c]	$C_{45}H_{71}O_{11}Na$	66.64	8.82
				(66.53	8.91)
f	+33.1 (0.33)	218—221[c]	$C_{46}H_{73}O_{11}Na$	66.96	8.92
				(66.70	9.03)
g	+31.7 (0.32)	220—223[c]	$C_{47}H_{75}O_{11}Na$	67.28	9.01
				(67.08	9.21)

a) Recrystallized from acetone–hexane. *b*) Colorless prisms. *c*) Colorless plates.

TABLE IX. Summary of Crystal Data and Intensity Collection Parameters for Na-**3e** and K-**3e**

	Na-**3e**·isopropylether	K-**3e**·acetone
Formula	$C_{45}H_{71}NaO_{11}\cdot(C_3H_7)_2O$	$C_{45}H_{71}KO_{11}\cdot(CH_3)_2CO$
F.W., amu	913.2	885.2
Crystal dimensions (mm^3)	0.27 × 0.30 × 0.63	0.30 × 0.42 × 0.72
Space group	$P2_12_12_1$	$P2_12_12_1$
Temperature (K)	295	295
a(Å)	10.029 (1)	10.248 (1)
b(Å)	16.650 (1)	16.220 (2)
c(Å)	30.278 (3)	30.338 (3)
V(Å^3)	5056.2 (8)	5043.1 (9)
Z	4	4
Calcd density (D_c, g/cm^3)	1.200	1.164
Radiation	Graphite-monochromated MoK_α	
2θ range (°)	3—50	3–50
Scan technique	$\omega-2\theta$	$\omega-2\theta$
Scan range (ω, °)	$0.75+0.35\tan\theta$	
Criterion for observation	$F_O>3\sigma$ (F_O)	$F_O>3\sigma$ (F_O)
Unique obsd data	2746	3063
R	0.087	0.063
Rw	0.092	0.065
No. of variables	555	553

tals of both compounds were sealed in a thin-walled capillary and were examined on an Enraf-Nonius CAD4 diffractometer using Mo/K_α radiation. A summary of the crystal data and the intensity collection for the two compounds is given in Table IX. Intensity data were corrected for Lorentz and polarization effects, but not for absorption. The structure of the K-**3e** molecule was solved by direct methods[9] and refined by difference Fourier and full-matrix least-squares techniques.[10] In an initial E-map some non-hydrogen atomic positions, including that of K, could be located. Subsequent difference Fourier syntheses revealed most non-hydrogen atomic positions of the molecule. After a few cycles of refinement with isotropic thermal factors, a difference Fourier map indicated 3 eq peaks for the C(45) carbon. These were assigned to C(45A), C(45B), and C(45C) with one-third occupancy. All non-hydrogen atoms of K-**3e** except for the C(45) carbons were refined with anisotropic thermal parameters, and positions with isotropic thermal factors as fixed parameters.

The structure of Na-**3e** was solved by the use of atomic positions of non-hydrogen atoms of K-**3e** as initial input into the structure-factor calculations. No disorder for the C(45) carbon was found in Na-**3e**, but a highly disordered solvent molecule was found in a subsequent difference Fourier map. For the disordered solvent, several carbon atoms were appropriately placed with an occupancy factor of 0.5 or 1.0 as a randomly orientated molecule; probably isopropyl ether. All non-hydrogen atoms of Na-**3e** except for the disordered solvent were refined with anisotropic

TABLE X. Positional Parameters and Their Estimated Standard Deviations of K-**3e**

Atom	x	y	z	B (A^2)[a]
K	0.6361 (2)	0.5511 (1)	0.83669 (7)	4.48 (5)
O(1)	0.4415 (7)	0.4020 (5)	0.8592 (2)	6.2 (2)
O(2)	0.397 (1)	0.4888 (5)	0.9129 (3)	8.3 (3)
O(3)	0.4750 (7)	0.2357 (5)	0.9717 (2)	6.7 (2)
O(4)	0.7560 (6)	0.4095 (3)	0.8167 (2)	3.9 (1)
O(5)	0.8379 (6)	0.4081 (4)	0.9323 (2)	4.4 (1)
O(6)	0.8310 (5)	0.5274 (3)	0.8897 (2)	3.6 (1)
O(7)	0.7703 (5)	0.6878 (3)	0.8644 (2)	3.7 (1)
O(8)	0.7299 (5)	0.6532 (3)	0.7739 (2)	3.5 (1)
O(9)	0.4703 (5)	0.6216 (3)	0.7726 (2)	3.5 (1)
O(10)	0.3926 (6)	0.4890 (3)	0.7845 (2)	4.1 (1)
O(11)	0.3922 (7)	0.6107 (4)	0.8581 (2)	5.9 (2)
C(1)	0.4142 (9)	0.4184 (7)	0.8976 (3)	5.0 (3)
C(2)	0.397 (1)	0.3470 (6)	0.9309 (3)	5.1 (2)
C(3)	0.515 (1)	0.2905 (6)	0.9374 (3)	4.9 (2)
C(4)	0.6458 (9)	0.3305 (6)	0.9520 (3)	4.6 (2)
C(5)	0.7241 (9)	0.3704 (6)	0.9132 (3)	4.1 (2)
C(6)	0.766 (1)	0.3089 (5)	0.8767 (3)	4.4 (2)
C(7)	0.8399 (9)	0.3572 (5)	0.8420 (3)	4.1 (2)
C(8)	0.9472 (8)	0.4102 (6)	0.9028 (3)	4.3 (2)
C(9)	0.9080 (8)	0.4594 (6)	0.9028 (3)	3.8 (2)
C(10)	1.0216 (9)	0.4973 (6)	0.9280 (3)	4.8 (2)
C(11)	0.960 (1)	0.5695 (6)	0.9513 (3)	5.3 (2)
C(12)	0.8462 (8)	0.5955 (5)	0.9203 (3)	3.8 (2)
C(13)	0.8754 (9)	0.6728 (6)	0.8941 (3)	4.3 (2)
C(14)	0.9951 (8)	0.6689 (7)	0.8637 (4)	5.6 (3)
C(15)	0.9560 (8)	0.7167 (6)	0.8220 (3)	4.5 (2)
C(16)	0.8145 (8)	0.7436 (5)	0.8313 (3)	4.0 (2)
C(17)	0.7185 (8)	0.7347 (5)	0.7931 (3)	3.6 (2)
C(18)	0.7244 (9)	0.7915 (5)	0.7535 (3)	4.4 (2)
C(19)	0.632 (1)	0.7454 (5)	0.7232 (3)	4.5 (2)
C(20)	0.6634 (8)	0.6545 (5)	0.7325 (3)	3.8 (2)
C(21)	0.5429 (8)	0.5981 (5)	0.7336 (3)	3.6 (2)
C(22)	0.4580 (9)	0.6033 (5)	0.6927 (3)	4.5 (2)
C(23)	0.3319 (9)	0.5551 (6)	0.7010 (3)	5.3 (2)
C(24)	0.2630 (8)	0.5825 (5)	0.7423 (3)	4.8 (2)
C(25)	0.3568 (8)	0.5726 (5)	0.7811 (3)	3.9 (2)
C(26)	0.3012 (9)	0.6048 (5)	0.8236 (3)	4.8 (2)
C(27)	0.1337 (9)	0.5357 (6)	0.7498 (4)	6.9 (2)
C(28)	0.530 (1)	0.5702 (7)	0.6519 (3)	6.8 (3)
C(29)	0.859 (1)	0.8007 (6)	0.7314 (3)	5.8 (3)
C(30)	0.810 (1)	0.8326 (6)	0.8488 (3)	5.4 (3)
C(31)	0.680 (1)	0.8577 (7)	0.8696 (4)	7.5 (3)
C(32)	0.719 (1)	0.6069 (7)	0.9460 (3)	5.4 (3)
C(33)	0.845 (1)	0.2362 (6)	0.8954 (4)	7.2 (3)
C(34)	0.626 (1)	0.3917 (7)	0.9895 (3)	6.1 (3)
C(35)	0.280 (1)	0.2952 (8)	0.9164 (4)	7.3 (3)
C(36)	0.533 (1)	0.1579 (8)	0.9717 (5)	9.2 (4)
C(37)	0.6821 (8)	0.3656 (5)	0.7844 (3)	4.4 (2)
C(38)	0.7294 (7)	0.3788 (4)	0.7388 (2)	3.2 (2)
C(39)	0.8163 (8)	0.4400 (6)	0.7278 (3)	4.6 (2)
C(40)	0.8527 (8)	0.4539 (6)	0.6844 (3)	5.4 (2)
C(41)	0.8039 (9)	0.4056 (7)	0.6502 (3)	5.2 (2)
C(42)	0.718 (1)	0.3438 (6)	0.6616 (3)	5.8 (3)
C(43)	0.6805 (8)	0.3313 (5)	0.7051 (3)	4.5 (2)
C(44)	0.841 (1)	0.419 (1)	0.6016 (4)	9.5 (4)
C(45A)	0.745 (1)	0.478 (1)	0.582 (1)	10 (1)
C(45B)	0.748 (3)	0.444 (2)	0.571 (1)	7 (1)
C(45C)	0.923 (4)	0.502 (2)	0.595 (1)	9 (1)
C(46)[b]	0.400 (2)	0.673 (2)	−0.0033 (7)	17 (1)
C(47)[b]	0.326 (3)	0.596 (2)	0.007 (1)	22 (1)
C(48)[b]	0.359 (2)	0.721 (1)	−0.0426 (6)	17.4 (8)
O(12)[b]	0.484 (1)	0.7023 (9)	0.0196 (4)	15.8 (5)

a) Anisotropically refined atoms are given in the form of the isotropic equivalent displacement parameter defined as: $(4/3)\times[a^2\times B(1,1)+b^2\times B(2,2)+c^2\times B(3,3)+ab(\cos\gamma)\times B(1,2)+ac(\cos\beta)\times B(1,3)+bc(\cos\alpha)\times B(2,3)]$. *b*) Atoms of acetone.

TABLE XI. Positional Parameters and Their Estimated Standard Deviations of Na-**3e**

Atom	x	y	z	B (A^2)[a]
Na	0.6481 (5)	0.5519 (3)	0.8284 (2)	4.0 (1)
O(1)	0.391 (1)	0.3873 (6)	0.8585 (3)	5.9 (3)
O(2)	0.375 (1)	0.4745 (6)	0.9126 (3)	5.8 (3)
O(3)	0.456 (1)	0.2334 (6)	0.9736 (3)	6.2 (3)
O(4)	0.7261 (8)	0.4068 (4)	0.8124 (3)	3.8 (2)
O(5)	0.8131 (9)	0.4041 (5)	0.9281 (3)	4.5 (2)
O(6)	0.8080 (8)	0.5203 (5)	0.8845 (3)	3.9 (2)
O(7)	0.7633 (8)	0.6736 (5)	0.8572 (3)	4.1 (2)
O(8)	0.7390 (8)	0.6364 (4)	0.7681 (3)	3.6 (2)
O(9)	0.4829 (7)	0.6037 (4)	0.7714 (3)	3.6 (2)
O(10)	0.410 (1)	0.4774 (5)	0.7880 (3)	5.3 (2)
O(11)	0.4353 (9)	0.5865 (6)	0.8592 (3)	4.9 (2)
C(1)	0.381 (1)	0.4045 (8)	0.8981 (4)	4.0 (3)
C(2)	0.363 (1)	0.3382 (9)	0.9322 (4)	5.1 (4)
C(3)	0.491 (1)	0.2845 (8)	0.9381 (4)	4.3 (3)
C(4)	0.623 (1)	0.3304 (9)	0.9501 (5)	5.2 (4)
C(5)	0.693 (1)	0.3667 (7)	0.9094 (4)	3.9 (3)
C(6)	0.733 (1)	0.3097 (7)	0.8726 (4)	4.0 (3)
C(7)	0.810 (1)	0.3546 (7)	0.8364 (4)	4.0 (3)
C(8)	0.925 (1)	0.4047 (7)	0.8565 (4)	3.7 (3)
C(9)	0.888 (1)	0.4501 (8)	0.8972 (4)	4.4 (3)
C(10)	1.004 (1)	0.4872 (9)	0.9225 (5)	5.3 (4)
C(11)	0.940 (1)	0.5578 (8)	0.9474 (5)	5.4 (4)
C(12)	0.828 (1)	0.5869 (7)	0.9163 (4)	3.8 (3)
C(13)	0.866 (1)	0.6608 (8)	0.8887 (5)	4.9 (4)
C(14)	0.992 (1)	0.6579 (8)	0.8598 (5)	4.5 (3)
C(15)	0.961 (1)	0.7022 (9)	0.8181 (5)	4.6 (3)
C(16)	0.812 (1)	0.7287 (7)	0.8237 (5)	4.4 (3)
C(17)	0.725 (1)	0.7161 (7)	0.7853 (4)	3.6 (3)
C(18)	0.733 (1)	0.7704 (7)	0.7447 (5)	4.6 (4)
C(19)	0.642 (1)	0.7228 (8)	0.7142 (5)	4.9 (4)
C(20)	0.669 (1)	0.6341 (7)	0.7261 (4)	4.3 (3)
C(21)	0.542 (1)	0.5818 (6)	0.7311 (4)	3.4 (3)
C(22)	0.448 (1)	0.5862 (7)	0.6919 (4)	4.3 (3)
C(23)	0.323 (1)	0.5409 (7)	0.7050 (4)	4.9 (3)
C(24)	0.263 (1)	0.5650 (7)	0.7486 (5)	4.5 (3)
C(25)	0.370 (1)	0.5585 (6)	0.7838 (4)	3.4 (3)
C(26)	0.334 (1)	0.5898 (7)	0.8285 (4)	4.5 (3)
C(27)	0.137 (1)	0.518 (1)	0.7590 (5)	7.3 (5)
C(28)	0.509 (2)	0.5552 (8)	0.6493 (4)	6.0 (4)
C(29)	0.870 (2)	0.780 (1)	0.7250 (6)	6.8 (5)
C(30)	0.805 (1)	0.8168 (7)	0.8420 (5)	5.0 (4)
C(31)	0.667 (2)	0.838 (1)	0.8590 (6)	7.6 (5)
C(32)	0.701 (1)	0.6007 (9)	0.9412 (5)	5.6 (4)
C(33)	0.813 (2)	0.2365 (8)	0.8897 (5)	6.6 (5)
C(34)	0.607 (2)	0.3861 (9)	0.9883 (4)	5.8 (4)
C(35)	0.247 (1)	0.2837 (9)	0.9185 (5)	6.3 (4)
C(36)	0.518 (3)	0.158 (1)	0.9715 (6)	10.2 (7)
C(37)	0.661 (1)	0.3634 (6)	0.7790 (4)	3.8 (3)
C(38)	0.720 (1)	0.3702 (6)	0.7344 (4)	3.2 (3)
C(39)	0.816 (1)	0.4257 (7)	0.7231 (4)	4.3 (3)
C(40)	0.858 (1)	0.4335 (8)	0.6802 (5)	5.0 (3)
C(41)	0.814 (1)	0.3866 (9)	0.6466 (4)	5.0 (3)
C(42)	0.717 (2)	0.3314 (9)	0.6577 (5)	5.8 (4)
C(43)	0.673 (1)	0.3227 (7)	0.7006 (4)	4.5 (3)
C(44)	0.854 (2)	0.397 (1)	0.5989 (5)	7.3 (5)
C(45)	0.775 (3)	0.452 (1)	0.5726 (6)	7.3 (5)
C(46)[b]	0.739 (6)	−0.021 (3)	0.966 (2)	11 (2)
C(47)[b]	0.788 (6)	−0.136 (3)	1.013 (2)	12 (1)
C(48)[b]	0.815 (5)	0.004 (3)	0.941 (1)	10 (1)
C(49)[b]	0.891 (7)	−0.185 (5)	1.010 (3)	14 (2)
C(50)[b]	0.832 (6)	−0.200 (4)	1.036 (2)	12 (2)
C(51)[b]	0.905 (6)	−0.242 (3)	1.024 (2)	12 (2)
C(52)[b]	0.807 (7)	−0.043 (4)	0.985 (2)	13 (2)
C(53)[b]	0.780 (6)	−0.116 (5)	0.987 (2)	26 (3)
C(54)[b]	0.856 (7)	−0.127 (5)	0.980 (3)	12 (2)

a) Anisotropically refined atoms are given in the form of the isotropic equivalent displacement parameter defined as: $(4/3) \times [a^2 \times B(1,1) + b^2 \times B(2,2) + c^2 \times B(3,3) + ab(\cos\gamma) \times B(1,2) + ac(\cos\beta) + B(1,3) + bc(\cos\alpha) \times B(2,3)]$. *b*) Isotropically refined atoms of isopropylether.

thermal parameters, and hydrogen atoms bound to carbon were included in the calculated positions as fixed parameters. Final cycles of two-blocked matrix least-squares refinement[10] for K-**3e** and Na-**3e** and were carried to convergence at $R = 0.063$ ($Rw = 0.065$)[11] and $R = 0.087$ ($Rw = 0.092$), respectively. The final difference Fourier maps were judged to be essentially featureless: the largest residual peaks of $0.3\, e/\text{Å}^3$ level were found near the C(31) carbon for K-**3e** and the O(4) oxygen for Na-**3e**. The atomic coordinates for non-hydrogen atoms with the isotropic equivalent thermal factors are given in Table X for K-**3e** and Table XI for Na-**3e**.[12]

Acknowledgment We thank Dr. K. Hirai and Ms. Y. Ishikawa of the Aichi Red Cross Blood Center for providing human blood, and Ms. T. Naito, Ms. K. Kato, Ms. T. Nakano and Ms. K. Takahashi of this faculty for elemental analysis, NMR and MS measurements. We also thank Dr. Y. Hotta and Prof. K. Takeya of Aichi Medical University for their advice on ^{23}Na-NMR measurement. This work was supported in part by a Grant-in-Aid for Scientific Research from the Ministry of Education, Science, and Culture of Japan, and a Grant from the Ishida Foundation.

References and Notes

1) *a*) C. Liu, "Polyether Antibiotics: Naturally Occurring Acid Ionophores," Vol. I, ed. by J. W. Westley, Marcel Dekker, New York, 1982, pp. 44—51; *b*) M. D. Ruff, "Polyether Antibiotics: Naturally Occurring Acid Ionophores," Vol. I, ed. by J. W. Westley, Marcel Dekker, New York, 1982, pp. 304—314.

2) E. N. Duesler, I. C. Paul, "Polyether Antibiotics: Naturally Occurring Acid Ionophores," Vol. II, ed. by J. W. Westley, Marcel Dekker, New York, 1982, pp. 170—178.

3) A. Nakamura, S. Nagai, T. Takahashi, R. Malhan, N. Murakami, T. Ueda, J. Sakakibara, M. Asano, *Chem. Pharm. Bull.*, **40**, 2331 (1992).

4) G. H. Coleman, C. R. Hauser, *J. Am. Chem. Soc.*, **50**, 1193 (1928).

5) *a*) G. L. Biagi, M. C. Guerra, A. M. Barbaro, *J. Med. Chem.*, **13**, 944 (1970); *b*) N. Shirai, J. Sakakibara, T. Kaiya, Y. Hotta, K. Takeya, *ibid.*, **26**, 851 (1983).

6) A. Nakamura, S. Nagai, T. Ueda, J. Sakakibara, Y. Hotta, K. Takeya, *Chem. Pharm. Bull.*, **37**, 2330 (1989).

7) W. L. Duax, G. D. Smith, P. D. Strong, *J. Am. Chem. Soc.*, **102**, 6725 (1980).

8) W. Pangborn, W. Duax, D. Langs, *J. Am. Chem. Soc.*, **109**, 2163 (1987).

9) Programs of the Enraf-Nonius SDP package were used. The package includes modified versions of Main, Hull, Lessinger, Germain, Declerq, and Woolfson's MULTAN82 and Johnson's ORTEP II.

10) The programs used in the refinement and the e.s.d. calculation were Scheidt and Haller's (Notre Dame) versions of ORFLS and ORFFE, originated by W. R. Busing, K. O. Martin, H. A. Levy.

11) The atomic scattering factors were taken from "International Tables for X-Ray Crystallography," Vol. IV, Kynoch Press, Birmingham (1974). $R = \Sigma \| F_O | - | F_C \| / \Sigma | F_O |$, $Rw = [\Sigma w(|F_O| - |F_C|)^2 / \Sigma w(F_O)^2]^{1/2}$ with unit weight.

12) Tables of the anisotropic temperature factors for non-hydrogen atoms, the idealized atomic coordinates for hydrogen atoms, the individual bond lengths and angles, and observed and calculated structure factors are available from the authors on request.